SCIENCE CHINA
Chemistry

•ARTICLES•

June 2023 Vol.66 No.6: 1714–1721
https://doi.org/10.1007/s11426-023-1584-y

Coordination cage with structural "defects" and open metal sites catalyzes selective oxidation of primary alcohols

Tian-Pu Sheng[1,3], Ying Wei[2], Parvathi Jampani[4], Chang Li[1,3], Feng-Rong Dai[1,3*], Shuping Huang[2*], Zhenqiang Wang[4*] & Zhong-Ning Chen[1,3*]

[1]*State Key Laboratory of Structural Chemistry, Fujian Institute of Research on the Structure of Matter, Chinese Academy of Sciences, Fuzhou 350002, China;*
[2]*College of Chemistry, Fuzhou University, Fuzhou 350108, China;*
[3]*University of Chinese Academy of Sciences, Beijing 100049, China;*
[4]*Department of Chemistry & Center for Fluorinated Functional Materials, University of South Dakota, Vermillion, SD, USA*

Received February 21, 2023; accepted March 27, 2023; published online May 10, 2023

Coordination cages with intrinsic enzyme-like activity are a class of promising catalysts for improving the efficiency of organic reactions. We present herein a viable strategy to conveniently construct multimetallic active sites into a coordination cage *via* self-assembly of a pre-formed sulfonylcalix[4]arene-based tetranuclear copper(II) precursor and an amino-functionalized dicarboxylate linker. The cage exhibits a "defective", partially open cylindrical structure and features coordinatively labile dimetallic Cu(II) sites. Modulated by this unique inner cavity environment, promising catalytic activity toward selective oxidation of primary alcohols to carboxylic acids at room temperature is achieved. Mechanistic studies reveal that the coordinatively labile dimetallic Cu(II) sites can efficiently capture and activate the substrate and oxidant to catalyze the reaction, while the confined nano-cavity environment modulates substrate binding and enhances the catalytic turnover. This study provides a new approach to designing biomimetic multifunctional coordination cages and environmentally friendly supramolecular catalysts.

coordination cages, open metal sites, alcohol oxidation, host-guest systems, supramolecular chemistry

Citation: Sheng TP, Wei Y, Jampani P, Li C, Dai FR, Huang S, Wang Z, Chen ZN. Coordination cage with structural "defects" and open metal sites catalyzes selective oxidation of primary alcohols. *Sci China Chem*, 2023, 66: 1714–1721, https://doi.org/10.1007/s11426-023-1584-y

1 Introduction

As a fundamental reaction in organic chemistry, oxidation of primary alcohols to carboxylic acids is considered as one of the most important processes in industrial manufacturing and of particular relevance in the preparation of biopharmaceutical intermediates [1,2]. Strong oxidants, such as Jones reagent or $KMnO_4$, are commonly and widely used to achieve such transformations, but they result in some serious problems, such as harsh reaction condition, poor reaction selectivity (*e.g.*, indiscriminate- or over-oxidation), complicated post-processing, and potential environmental hazards. To circumvent these issues, metal-based catalysts combined with milder oxidants (*e.g.*, sodium hypochlorite, hydrogen peroxide, *tert*-butyl hydroperoxide) have been developed [3–7], though limitations persist due to the use of precious metals, high reaction temperature, and other additional stringent requirements in these alternative methods. Therefore, the development of highly efficient, environmentally friendly, and low-cost catalysts for selective alcohol oxidation remains an attractive but challenging task.

*Corresponding authors (email: dfr@fjirsm.ac.cn; huangshp@gmail.com; Zhenqiang.Wang@usd.edu; czn@fjirsm.ac.cn)

Supramolecular architectures with intrinsic enzyme-like activity have attracted considerable attention owing to their uniquely tunable catalytic activity and their potential applications in chemical transformations relevant to biomedicine, industrial manufacturing, and environmental remediation [8–12]. Coordination cages, a particular type of supramolecular assemblies that are sustained by coordination bonds between metal centers and organic linkers, have shown excellent potential in imitating enzymatic catalysis thanks to their restricted nanocavity microenvironment and synergistic chemical functionalities tunable through modification to the metal ions and/or the organic linkers [13–20]. A common approach to introducing catalytic moieties to a coordination cage is *via* covalent modification of the organic linker, which may require tedious or even impractical synthetic protocols that are incompatible with the cage structure [21]. By contrast, incorporating open metal sites into the coordination cages could be a more effective approach to constructing suitable catalytic sites. Indeed, generating open metal sites has become a widely adopted strategy to functionalize metal-organic frameworks (MOFs) and obtain catalytic activity [22,23], although such studies are often limited to Lewis-acid-based catalysis. Notably, this strategy has not yet been fully understood within the context of coordination cages. Several recent examples of coordination cages [24–26] with structural "defects" suggest that deliberate removal of one or more organic linkers in a coordination cage not only leads to large pore opening, which facilitates substrate/product exchange, but also generates coordinatively labile metal site(s) suitable for catalysis.

To this end, we report herein the rational design of a copper (II) coordination cage (**1**, Scheme 1) with exceptional biomimetic catalysis towards selective oxidation of primary alcohols. Coordination cages constructed from $M_4(\mu_4\text{-X})$ tetranuclear units (where M is a divalent metal ion and X can be Cl^- or O^{2-}) capped by sulfonylcalix[4]arenes and linked by polydentate carboxylate ligands represent a unique family of supramolecular host molecules [27–35]. Although an array of divalent metal ions, including Co(II), Ni(II), Zn(II), and Mg(II), have been utilized to construct these coordination cages, we reasoned that choice of Cu(II) could present a unique entry into the design of biomimetic catalysts for alcohol oxidation. Coordination cage **1** was assembled from the reaction of a **Cu_4TBSC** (TBSC = *p*-*tert*-butylsulfonylcalix[4]arene) tetranuclear precursor and an amine-containing dicarboxylate linker (Scheme 1). Cage **1** features multifunctional characteristics desired for a biomimetic catalyst, including coordinatively labile Cu^{2+} centers, Lewis-basic –NH– sites, and a well-defined cylindrical *endo* cavity with a large opening to accommodate substrate/product exchange. Indeed, cage **1** showed encouraging attributes as a highly efficient, selective, and green catalyst for the oxidation of primary alcohols to carboxylic acids, achieving the oxidation cleanly and selectively under environmentally benign conditions, namely, at room temperature, use of a mild oxidant (*tert*-butyl hydroperoxide, TBHP), and without any additional additives such as a strong acid or base. The superb performance of cage **1** for the oxidation of primary alcohols can be attributed in part to its uniquely tuned binding characteristics toward the three key molecules in the reaction sequence, namely, alcohol substrate, aldehyde intermediate, and carboxylic acid product, with the binding affinity descending in the order of alcohol > aldehyde > carboxylic acid.

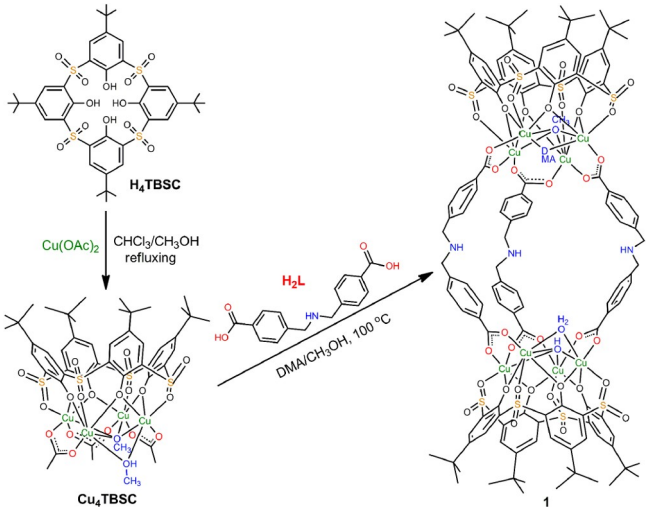

Scheme 1 Self-assemblies of **Cu_4TBSC** precursor and coordination cage **1** (color online).

2 Experimental

2.1 Synthesis of cage 1

H_2**L** (21.37 mg, 0.075 mmol) and **Cu_4TBSC** precursor (68.00 mg, ~0.05 mmol) were dissolved in a mixture solvent of dimethylacetamide (DMA) (5 mL) and methanol (3 mL) in a glass vial (20-mL capacity). The vial was placed in a sand bath, which was transferred to a programmable oven and heated at a rate of 0.5 °C/min from 30 to 100 °C. The temperature was held at 100 °C for 24 h before the oven was cooled at a rate of 0.2 °C/min to a final temperature of 30 °C. Green crystals of **1** were obtained, and isolated by filtration. After washing with DMF and acetone for five times, the crystals were soaked in fresh acetone for 3 days during which the solvent was replenished for five times. The crystals were then vacuum-dried at 100 °C to give rise to 25.13 mg of activated material. Yield: 10.47%. FT-IR (KBr): ν = 2,959 (m), 1,609 (vs), 1,488 (vs), 1,418 (s), 1,266 (s), 1,135 (m), 1,081 (s), 798 (s), 559 (vs) cm^{-1}. Anal. Calcd. for $C_{133}H_{141}Cu_8N_4O_{40}S_8$: C, 49.91; H, 4.44; N, 1.75%. Found: C, 49.01; H, 4.20; N, 1.94%.

2.2 Cage 1-catalyzed oxidation reactions

Aromatic alcohols (0.1 mmol), 70% TBHP solution (0.5 mmol), and cage **1** (3 mol%) were suspended in CD_3CN (1 mL), which was stirred at room temperature for 12 h. After the reaction, excess sodium thiosulfate was added to the solution, and the obtained mixture was then centrifuged for three times. The supernatant was collected and concentrated for ^{1}H nuclear magnetic resonance (^{1}H NMR) studies to determine the reaction conversion and purity of the products.

2.3 Recycling performance

After each reaction, 20 mL ether was added to the mixture. Cage **1** was collected by centrifuge, washed with methanol and acetone for three times, and soaked in fresh acetone for 2 h. Finally, the collected cage **1** was dried in a vacuum at 60 °C for 12 h, and used for the next cycle of catalytic reaction.

2.4 Host-guest chemistry

The solution host-guest chemistry was probed using the ultraviolet-visible (UV-vis) titration technique. Stock solutions of the cage **1** were prepared in DMA at a concentration of ~5×10^{-6} M. Then, 10.00 mL of the stock solution was used to dissolve the samples of benzyl alcohol, benzoic aldehyde, or benzoic acid, chosen to yield a solution at a concentration 100 times greater than that of the host. Subsequently, 2.00 mL of the cage **1** solution was placed in a 10.0 mm quartz cell, upon which 0.005–0.2 mL of the benzyl alcohol, benzoic aldehyde, or benzyl acid solution was added gradually. After each addition, the cell was stoppered and inverted, and the UV-vis spectrum was collected (at 25 °C) after 5 min to ensure complete mixing and reaching equilibration. To evaluate the overall binding strength, the titration results were fitted to the non-linear Hill equation [36,37]: where ΔA ($= A - A_0$) is the change in absorption intensity, $[H]_0$ is the initial cage concentration, K_a is the association constant, and n is the Hill coefficient. A plot of ΔA against $[H]_0$ can be used to estimate the values of ΔA_{max}, n, and K_a.

$$\frac{\Delta A}{\Delta A_{max}} = \frac{K_a{}^n[H]_0{}^n}{1+K_a{}^n[H]_0{}^n} \quad (1)$$

3 Results and discussion

3.1 Synthesis and structure

Coordination cage **1** was prepared through a two-step reaction as depicted in Scheme 1. The tetranuclear copper(II) cluster (**Cu_4TBSC**) was first synthesized from the reaction of *p-tert*-butyl-sulfonylcalix[4]arene (H_4TBSC) and $Cu(AcO)_2$ in a mixture solvent of chloroform and methanol under reflux for 6 h. The **Cu_4TBSC** precursor was then combined with a flexible dicarboxylate ligand (H_2**L**) in a mixture solvent of *N*, *N*′-dimethylacetamide (DMA) and methanol, which was heated at 100 °C for 24 h to afford the green crystalline material of **1**. The purity of the obtained product **1** was confirmed by power X-ray diffraction and Fourier transform IR spectroscopy (Figures S1–S3, Supporting Information online), while thermogravimetric analysis indicates its excellent thermal stability (Figures S4 and S5). The oxidation state of copper in cage **1** are +2 as determined by the XPS studies (Figures S7–S9).

Slow diffusion of methanol into the DMA solution of **Cu_4TBSC** gave rise to single crystals suitable for single crystal X-ray diffraction (SCXRD) analysis. As shown in Figure 1a, complex **Cu_4TBSC** adopts a C_s symmetry and consists of one deprotonated TBSC, four Cu^{2+} ions, three acetate anions, one deprotonated methoxide (μ_4-OCH_3), and a neutral methanol molecule (μ_2-$OHCH_3$) substituting the missing carboxylate linker. There are two coordinatively distinct types of Cu(II) ions. In both cases, the copper ions display an octahedral coordination geometry, and each Cu(II) ion is coordinated by two phenoxo O atoms and one sulfonyl O atom from TBSC, and one O atom from the deprotonated μ_4-OCH_3; Cu1 is further coordinated with two acetate anions, while Cu2 is coordinated with one O atom from an acetate anion and another O atom from μ_2-$OHCH_3$. The μ_2-$OHCH_3$ on the Cu2 centers is labile and can potentially be removed through a well-established activation procedure to afford desired open metal sites [23]. Notably, the deprotonated μ_4-OCH_3 clearly deviates from the central axis of the Cu_4 cluster and positions much closer to the Cu2 active sites, as in-

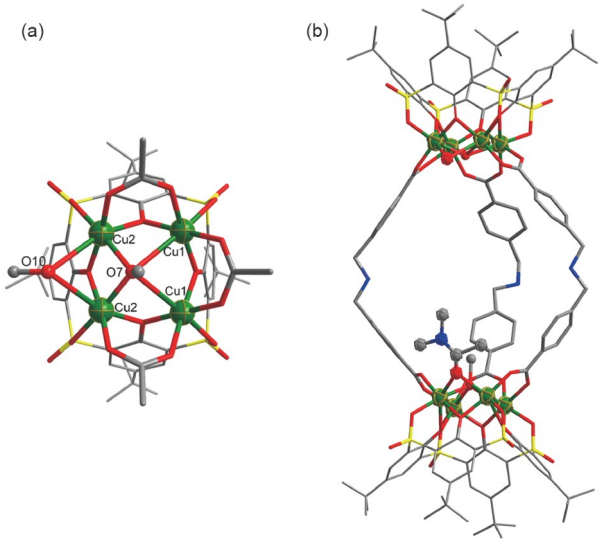

Figure 1 Crystal structures of **Cu_4TBSC** precursor (a) and cage **1** (b). Hydrogen atoms are omitted for clarity (color online).

dicated by the markedly shorter Cu2···O7(μ_4-OCH_3) distance (1.954(3) Å) than the Cu1···O7(μ_4-OCH_3) distance of 2.609(4) Å.

The SCXRD analysis revealed that the coordination cage **1** is consisted of two **Cu_4TBSC** tetranuclear clusters adopting a coordination geometry similar to the precursor. The **Cu_4TBSC** complexes are linked by three units of the dicarboxylate linker **L** that replace the acetate groups, and coordinated by one edge-bridging solvent molecule (water or DMA) and one face-bridging deprotonated solvent (OH^- or CH_3O^-), forming a partially open cylindrical cage [33,38,39] (Figure 1b). Cage **1** has an outer dimension of ca. 3.0 nm × 1.4 nm × 1.4 nm, an inner cavity with a diameter of ca. 1.1 nm, and a large pore opening (ca. 0.9 nm × 0.8 nm). Such a unique cavity and pore-opening architecture is crucial for efficient and selective encapsulation of reaction substrates and exclusion of reaction products, key to accelerating the catalytic cycle. The size and monodispersity of cage **1** were further confirmed by transmission electron microscope (TEM) analysis, which revealed a dimension of ca. 3 nm (Figure S10), consistent with that revealed by the X-ray crystal structure analysis.

3.2 Catalytic activity

The tri-functional characteristics of cage **1**, including its Lewis-base NH-sites, unique pore opening, and coordinatively labile Cu(II) sites, prompted us to reason that it could serve as a new family of "green" catalysts for alcohol oxidation [40,41]. The catalytic activity of **1** was examined against the oxidation of a series of primary alcohols (Scheme 2). After selecting *tert*-butyl hydroperoxide (TBHP) as the oxidant and screening the oxidant loading from 3 to 5 equiv. in different solvents (Tables S2 and S3, Supporting Information online), the optimized catalytic conditions were found to be 3 mol% of cage **1** and 5 equiv. of TBHP in acetonitrile at room temperature.

Cage **1** exhibited excellent catalytic activity for the oxidation of benzyl alcohol (**2a**) to benzoic acid (**4a**), affording a high conversion (95% yield, entry 1, Table 1) after 12 h. Interestingly, substituting benzyl alcohol with the electron-donating methoxy group (**2c**) led to nearly quantitative formation of the carboxylic acid product (99% yield, entry 3, Table 1). Similarly, primary alcohols with a larger aromatic substituent such as 1- and 2-naphthylcarbinol (**2d** and **2e**) also afforded the corresponding carboxylic acid products **4d** and **4e** nearly quantitatively (99% yield, entries 4 and 5, Table 1). These results indicate that electron-rich substituents such as methoxy group and extended π-systems likely contribute to strengthening π···π interactions between the cage (**1**) and the substrate, thereby enhancing the reaction efficacy and selectivity. Oxidation of heteroaromatic alcohols such as 2-furanmethanol (**2f**) and 2-thiophenemethanol (**2g**) also

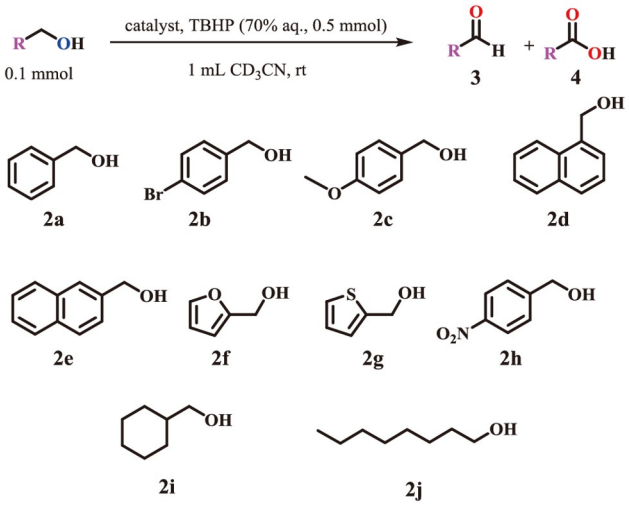

Scheme 2 Reaction scheme of the oxidation reaction and the alcohol substrates used in this study (color online).

produced the corresponding acid products **4f** and **4g**, respectively, in good yields (>90%, entries 6 and 7, Table 1).

In stark contrast, substituting benzyl alcohol with the electron-withdrawing nitro group (**2h**) gave rise to notably poorer reactivity and reaction selectivity, affording the aldehyde (**3h**) as the major product (74% yield) and carboxylic acid (**4h**) as a minor product (19% yield, entry 8, Table 1). These findings indicate that the nanocavity of cage **1** is uniquely suited for differentiating electron-rich substrates from electron-deficient ones, promoting a complete oxidation to the carboxylic acid product only for the former, likely through stronger π···π interactions between aromatic alcohol (substrate) and cage **1** (catalyst) (*vide infra*). Because the oxidation of alcohols to aldehydes first and then carboxylic acids is a successive electron loss process, it is reasonable to anticipate that electron-rich substrates such as 4-methoxybenzyl alcohol, 2-furanmethanol and 2-thiophenemethanol are more poised to be oxidized to carboxylic acid products than those of electro-deficient substrates such as 4-nitrobenzyl alcohol. The importance of π···π interactions in the selective oxidation was further evidenced by a notable lack of reactivity for alkyl alcohols such as cyclohexanemethanol (**2i**) and 1-octanol (**2j**), which underwent negligible oxidation reaction in the presence of cage **1** (entries 9 and 10, Table 1). Thus, supramolecular catalyst **1** exhibits excellent catalytic selectivity toward different types of primary alcohols under mild conditions, wherein the electron-rich aromatic primary alcohols can be effectively and fully oxidized to the corresponding carboxylic acids, while substituting the substrates with electron-withdrawing or electron-deficient moieties such as nitro groups led to the corresponding aldehydes as major products.

Experiments using the **Cu_4TBSC** precursor as a control catalyst were also performed to shed light on the importance

Table 1 Yields for oxidation reaction of alcohols catalyzed by cage **1**, **Cu_4TBSC** or ligand dimethyl ester (Me_2**L**)

Entry	Substrates	Yield (%) [a]							
		1 [b]		**Cu_4TBSC** [c]		Me_2**L** [d]		Blank	
		 3	 4	 3	 4	 3	 4	 3	 4
1 [e]	 2a	4	95	7	<1	<1	<1	<1	<1
2 [e]	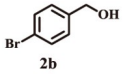 2b	2	97	25	<1	<1	<1	<1	<1
3 [f]	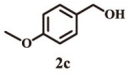 2c	1	99	16	3	<1	<1	<1	<1
4 [e]	 2d	<1	99	27	<1	<1	<1	<1	<1
5 [e]	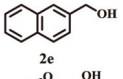 2e	<1	99	32	55	<1	<1	<1	<1
6 [e]	 2f	9	90	<1	<1	<1	<1	<1	<1
7 [e]	 2g	7	92	49	<1	<1	<1	<1	<1
8 [e]	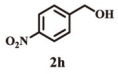 2h	74	19	52	19	<1	<1	<1	<1
9 [e]	 2i	<1	<1	<1	<1	<1	<1	<1	<1
10 [e]	 2j	<1	<1	<1	<1	<1	<1	<1	<1

a) Quantified by ^{1}H NMR spectra; b) 3 mol% of **1** was used; c) 6 mol% of **Cu_4TBSC** was used; d) 9 mol% of Me_2**L** was used; e) reaction time: 12 h; f) reaction time: 4 h.

of the cage architecture of **1** in the oxidation reactions. As listed in Table 1, **Cu_4TBSC** showed a notably poorer reactivity and selectivity, generally giving rise to aldehydes as the major products in significantly lower yields. Importantly, no noticeable oxidation products were found when the reactions were carried out in the presence of the dimethyl ester of the linker (Me_2**L**) or in the absence of a catalyst. Taken together, these findings suggest that the coordinatively labile copper(II) sites are likely responsible for facilitating the conversion of alcohols to aldehyde intermediates, while the unique microenvironment of the *endo* cavity, and/or the Lewis-basic –NH sites play a crucial and subtle role in modulating the further transformation of aldehydes to carboxylic acids, since **Cu_4TBSC** possesses similar copper sites but lacks the bridging linker or *endo* cavity present in cage **1**.

Additional efforts were made to replace TBHP with H_2O_2 as the oxidant, as the latter is considered a more environmentally friendly reagent due to its generation of H_2O as the only by-product. As listed in Table S4, the oxidation of benzyl alcohol (**2a**) took place in the presence of catalyst **1** and H_2O_2, resulting in an even higher reaction selectivity, and forming exclusively the fully oxidized carboxylic acid product (**4a**). It is worth noting that compared with TBHP, the use of H_2O_2 as the oxidant required a significantly shorter reaction time (6 *vs*. 12 h), but much higher (40 *vs*. 5) equiv. of the oxidant to achieve a slightly lower yield (81% *vs*. 95%). The results indicated that the cage **1** catalyst system is suitable for alcohol oxidation under mild condition with choices of environmentally friendly oxidants.

Another important consideration was to evaluate the recyclability of cage **1** as an alcohol oxidation catalyst. It should be noted that cage **1** was insoluble in acetonitrile and thus served as a heterogeneous catalyst. Catalyst **1** was thus collected by centrifuge after the reaction, rinsed with methanol and acetone, and soaked in fresh acetone for 2 h. The collected cage **1** material was then reactivated under vacuum

at 60 °C for 6 h and used for additional cycles of catalytic reactions. It was found that cage **1** maintained excellent catalytic activity after at least four cycles of oxidation using benzyl alcohol (**2a**) as the substrate (Figure 2a). The stability of the cage **1** catalyst after four recycles was confirmed by PXRD, UV-vis and FT-IR spectroscopic analysis (Figures S11–S13). The excellent recyclability and stability of this supramolecular catalyst demonstrate its promising application in practical settings such as industrial manufacturing.

3.3 Catalytic mechanism

To better understand the catalytic mechanism of the alcohol oxidation, host-guest binding of cage **1** with the benzyl alcohol substrate (**2a**), benzaldehyde intermediate (**3a**), and benzoic acid product (**4a**) was conducted using UV-vis spectroscopic titration experiments (Figures S14–S19). The binding constants of the three guests were calculated by fitting the titration data to the Hill equation [36] and were summarized in Table S5. The benzyl alcohol substrate (**2a**) exhibited the largest apparent association constant of $(4.17 \pm 0.15) \times 10^4$ with the Hill coefficient of $n = 2.40$, suggesting relatively strong and positively cooperative binding between **2a** and **1**. The binding affinity between benzoic aldehyde (**3a**) and **1** was calculated to be $(2.51 \pm 0.27) \times 10^4$, notably lower than that of alcohol substrate **2a** but higher than that of benzoic acid (**4a**), which was calculated to be $(1.54 \pm 0.56) \times 10^4$. These results indicate that the reaction substrate was able to access the inner cavity in a competitively favorable manner, contributing to increasing the local concentration of the substrate and promoting the reaction. On the other hand, since the fully oxidized carboxylic acid as the formed product appears to be the weakest guest, it can be envisioned to be readily replenished by the alcohol substrate, resulting in accelerated catalytic turnovers.

As illustrated in the crystal structure (Figure 1b), cage **1** possesses coordinatively labile copper sites that could be beneficial for immobilizing and activating the reaction substrate and the oxidant. The interaction models between cage **1** and substrate benzyl alcohol (**2a**) or oxidant TBHP were simulated using the density functional theory (DFT) calculations based on the PBE0 [42] functional and the DFT-D3 dispersion correction with Becke-Jonson damping [43]. As shown in the optimized structures (Figure 2b and Figure S20), the benzyl alcohol (**2a**) binds to cage **1** through the two coordinatively labile copper ions in an edge-bridging fashion to form a **2a**@**1** complex. Notably, the benzene ring of substrate **2a** adopts two possible orientations, one in parallel with an aromatic ring of TBSC unit (Figure 2b) and the other extended into the inner cavity and in parallel with an aromatic ring of the linker (Figure S20). The **2a**@**1** complex is thus stabilized through π···π interactions between the benzene rings of **2a** and TBSC or **L** ligands. The oxidant TBHP is also a suitable guest that binds to the Cu_4 cluster in an edge-bridging manner with the *tert*-butyl unit pointing inside the inner cavity of cage **1** (Figure S21). Such interactions are conducive to the generation of reactive species *via* the open copper active sites, thus facilitating subsequent oxidation reaction. A substantive evidence supporting the notion that cage **1** encapsulates and stabilizes reactive species came from an electron paramagnetic resonance (EPR) spectroscopic study, which captured a snapshot of the transient *tert*-butylperoxy radical (derived from the decomposition of TBHP) arrested by cage **1** catalyst in the presence of the known radical-trapping reagent 5,5-dimethyl-1-pyrroline-*N*-oxide (DMPO) (Figure 2c). Taking into consideration the catalytic reactivity of the **Cu_4TBSC** precursor (Table 1), it was evident that the pre-designed coordinatively labile Cu(II) sites play a crucial role in the catalytic oxidation reaction of alcohol into aldehyde.

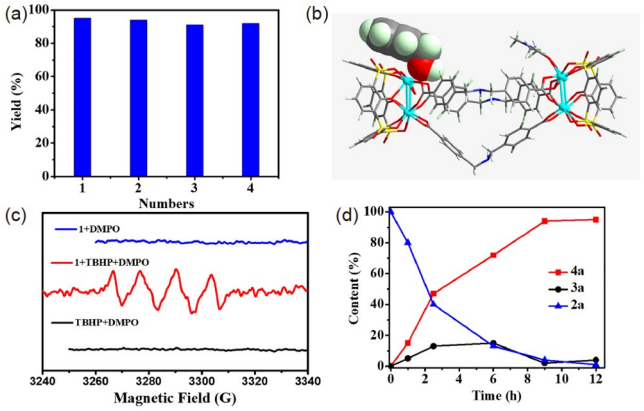

Figure 2 (a) Recycling performance of cage **1** for oxidizing benzyl alcohol (**2a**) into benzoic acid (**3a**). (b) Structural model obtained from the computational studies suggesting benzyl alcohol (**2a**) binding to cage **1** with the benzene ring of substrate **2a** in parallel to the surface of TBSC ligand. (c) EPR spectra of the mixture of **1** + DMPO (blue line), **1** + TBHP + DMPO (red line), and TBHP + DMPO (black line) in CH_3CN. (d) Time-dependent reaction profiles for oxidation of benzyl alcohol catalyzed with **1**. Yields were determined by ^{1}H NMR (color online).

To shed further light on the catalytic pathway, the kinetics of the oxidation reactions were studied (Figure 2d and Figures S22–S28). As shown in Figure 2d, the time-dependent reaction profiles of benzyl alcohol (**2a**) oxidation catalyzed by cage **1** revealed that the oxidation reaction proceeds immediately, giving rise to both benzoic acid (**4a**) and benzaldehyde (**3a**) at a ratio of ca. 3:1 within the first 2 h, suggesting that complete oxidation of alcohol to the acid took place through the aldehyde intermediate. A continuously rapid formation of carboxylic acid product accompanied by a somewhat constant level of the aldehyde was observed within 3–6 h. With continuous consumption of the aldehyde intermediate, the formation of benzoic acid (**4a**) further progressed after 6 h, resulting in the exclusive pro-

duction of product **4a** in 95% yield after 9 h. The kinetic studies thus confirmed the catalytic oxidation pathway of transformation from alcohol to aldehyde, and then the final carboxylic acid product.

The importance of the inner cavity was clearly demonstrated by comparing the oxidation reactivity of cage **1** to that of **Cu_4TBSC** precursor (*vide supra*). While the use of cage **1** produced almost exclusively the fully oxidized carboxylic acid products, **Cu_4TBSC** mainly afforded the partially oxidized aldehydes. Compared with cage **1**, **Cu_4TBSC** possesses a nearly identical tetranuclear architecture with similar copper(II) sites, but lacks an "*inner*" cavity surrounding the $Cu_4(\mu_4\text{-O})$ functional units. Therefore, it is not untenable to conclude that the microenvironment of the inner cavity in cage **1** was crucial in modulating the complete oxidation of aldehyde intermediates into the carboxylic acid products.

Based on the above discussion, a plausible mechanism for the cage **1**-catalyzed alcohol oxidation is proposed and shown in Scheme 3. An initial step involves the alcohol substrate and TBHP simultaneously interacting with the Cu_4 clusters, likely on opposing sides, which activates both and generates the benzyloxy anion and *tert*-butylperoxy radicals, respectively, by the copper active sites. These activated species are temporarily trapped and accumulated inside the inner cavity of cage **1** to allow the initial oxidation of the alcohol to the aldehyde to proceed. The aldehyde intermediate is subsequently oxidized by a second *tert*-butylperoxy radical within the inner cavity, giving rise to the desired carboxylic acid product which is subsequently rejected from the inner cavity due to the competition from the alcohol substrate and/or aldehyde intermediate as a result of its lower binding affinity with cage **1** than that of the latter two.

4 Conclusions

We have demonstrated the design of a supramolecular catalyst that exhibits exciting characteristics for selective alcohol oxidation. The new catalyst is based on a coordination cage (**1**) assembled from a pre-formed sulfonylcalix[4]arene-supported tetranuclear copper(II) cluster (**Cu_4TBSC**). Cage **1** exhibits a trademark multi-functional characteristic, reminiscent of a typical enzyme active site. It adopts an unusual "defective" cylindrical topology, characterized by an inner cavity that is surrounded by aromatic walls but features a wide pore opening due to a missing carboxylic linker. In addition to the potentially beneficial Lewis-basic –NH sites, cage **1** contains catalytically active dimetallic Cu(II) centers serving as an anchoring point for immobilizing and activating both the alcohol substrate and the oxidant. Taking advantage of these unique structural characteristics, cage **1** shows excellent and selective catalytic activity towards the oxidation of primary alcohols to carboxylic acids. We anticipate that this new family of coordination cages may find a broader range of synthetic applications as green and biomimetic-based supramolecular catalysts.

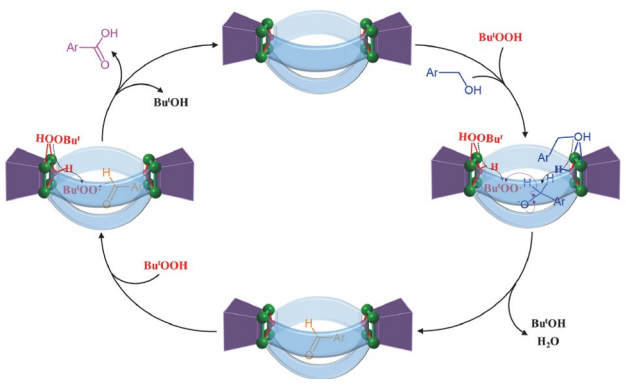

Scheme 3 Proposed mechanism for the oxidation reaction of primary alcohols catalyzed by **1** (color online).

Acknowledgements This work was supported by the National Natural Science Foundation of China (21673239, 92061202, U22A20387), the Fujian Science and Technology Project (2020L3022), and the Science and Technology Service Network Initiative (STS) Foundation of Fujian Provincial Department of Science and Technology (2021T3004). Z.W. and P.J. acknowledge the financial support provided by the National Science Foundation (CHE-1800354) and the South Dakota Governor's Office of Economic Development through the Center for Fluorinated Functional Materials (CFFM).

Conflict of interest The authors declare no conflict of interest.

Supporting information The supporting information is available online at chem.scichina.com and link.springer.com/journal/11426. The supporting materials are published as submitted, without typesetting or editing. The responsibility for scientific accuracy and content remains entirely with the authors.

1 Caron S, Dugger RW, Ruggeri SG, Ragan JA, Ripin DHB. *Chem Rev*, 2006, 106: 2943–2989
2 Gabriel T, Fernández M. *Oxidation of Primary Alcohols to Carboxylic Acids. Basic Reactions in Organic Synthesis*. New York: Springer, 2006
3 Rafiee M, Konz ZM, Graaf MD, Koolman HF, Stahl SS. *ACS Catal*, 2018, 8: 6738–6744
4 Cherepakhin V, Williams TJ. *Synthesis*, 2020, 53: 1023–1034
5 Greco R, Tiburcio-Fortes E, Fernandez A, Marini C, Vidal-Moya A, Oliver-Meseguer J, Armentano D, Pardo E, Ferrando-Soria J, Leyva-Pérez A. *Chem Eur J*, 2022, 28: e202103781
6 Nandi J, Hutcheson EL, Leadbeater NE. *Tetrahedron Lett*, 2021, 63: 152632
7 Zhou J, Huang-Fu X, Huang YY, Cao CN, Han J, Zhao XL, Chen XD. *Inorg Chem*, 2020, 59: 254–263
8 Lehn JM. *Supramolecular Chemistry*. Weinheim: VCH Publishing, 1995
9 Marchetti L, Levine M. *ACS Catal*, 2011, 1: 1090–1118
10 Ferrand Y, Crump MP, Davis AP. *Science*, 2007, 318: 619–622
11 Hooley RJ. *Nat Chem*, 2016, 8: 202–204
12 Raynal M, Ballester P, Vidal-Ferran A, van Leeuwen PWNM. *Chem Soc Rev*, 2014, 43: 1734–1787
13 Castilla AM, Ramsay WJ, Nitschke JR. *Acc Chem Res*, 2014, 47: 2063–2073

14 Stang PJ, Cao DH. *J Am Chem Soc*, 1994, 116: 4981–4982
15 Takezawa H, Kanda T, Nanjo H, Fujita M. *J Am Chem Soc*, 2019, 141: 5112–5115
16 Yoshizawa M, Tamura M, Fujita M. *Science*, 2006, 312: 251–254
17 Holloway LR, Bogie PM, Lyon Y, Ngai C, Miller TF, Julian RR, Hooley RJ. *J Am Chem Soc*, 2018, 140: 8078–8081
18 Guo J, Xu YW, Li K, Xiao LM, Chen S, Wu K, Chen XD, Fan YZ, Liu JM, Su CY. *Angew Chem Int Ed*, 2017, 56: 3852–3856
19 Wang QQ, Gonell S, Leenders SHAM, Dürr M, Ivanović-Burmazović I, Reek JNH. *Nat Chem*, 2016, 8: 225–230
20 Cullen W, Misuraca MC, Hunter CA, Williams NH, Ward MD. *Nat Chem*, 2016, 8: 231–236
21 Ueda Y, Ito H, Fujita D, Fujita M. *J Am Chem Soc*, 2017, 139: 6090–6093
22 Cai G, Jiang HL. *Angew Chem Int Ed*, 2017, 56: 563–567
23 Kökçam-Demir Ü, Goldman A, Esrafili L, Gharib M, Morsali A, Weingart O, Janiak C. *Chem Soc Rev*, 2020, 49: 2751–2798
24 Tang X, Chu D, Gong W, Cui Y, Liu Y. *Angew Chem Int Ed*, 2021, 60: 9099–9105
25 Li RJ, Tessarolo J, Lee H, Clever GH. *J Am Chem Soc*, 2021, 143: 3865–3873
26 Chen B, Holstein JJ, Horiuchi S, Hiller WG, Clever GH. *J Am Chem Soc*, 2019, 141: 8907–8913
27 Dai FR, Wang Z. *J Am Chem Soc*, 2012, 134: 8002–8005
28 He C, Sheng T-P, Dai F-R, Chen Z-N. *Chinese J Struct Chem*, 2020, 39: 2077–2084
29 Bi Y, Du S, Liao W. *Coord Chem Rev*, 2014, 276: 61–72
30 Sheng TP, He C, Wang Z, Zheng GZ, Dai FR, Chen ZN. *CCS Chem*, 2022, 4: 1098–1107
31 Chen X, Li C, Cao X, Jia X, Chen X, Wang Z, Xu W, Dai F, Zhang S. *Theranostics*, 2022, 12: 3251–3272
32 Qiao Y, Zhang L, Li J, Lin W, Wang Z. *Angew Chem Int Ed*, 2016, 55: 12778–12782
33 Dai FR, Qiao Y, Wang Z. *Inorg Chem Front*, 2016, 3: 243–249
34 Jiao J, Li Z, Qiao Z, Li X, Liu Y, Dong J, Jiang J, Cui Y. *Nat Commun*, 2018, 9: 4423
35 Fang Y, Xiao Z, Li J, Lollar C, Liu L, Lian X, Yuan S, Banerjee S, Zhang P, Zhou HC. *Angew Chem Int Ed*, 2018, 57: 5283–5287
36 Weiss JN. *FASEB J*, 1997, 11: 835–841
37 Hill AV. *J Physiol*, 1910, 40: iv–vii
38 Bhuvaneswari N, Annamalai KP, Dai FR, Chen ZN. *J Mater Chem A*, 2017, 5: 23559–23565
39 Bhuvaneswari N, Dai FR, Chen ZN. *Chem Eur J*, 2018, 24: 6580–6585
40 Sheldon RA, Arends IWCE, ten Brink GJ, Dijksman A. *Acc Chem Res*, 2002, 35: 774–781
41 Marais L, Swarts AJ. *Catalysts*, 2019, 9: 395
42 Adamo C, Barone V. *J Chem Phys*, 1999, 110: 6158–6170
43 Grimme S, Ehrlich S, Goerigk L. *J Comput Chem*, 2011, 32: 1456–1465